Int. J. Heat Mass Transfer. Vol. 8, pp. 887–904. Pergamon Press 1965. Printed in Great Britain

THE MECHANISM OF HEAT TRANSFER IN NUCLEATE POOL BOILING—PART I

BUBBLE INITIATON, GROWTH AND DEPARTURE

CHI-YEH HAN* and PETER GRIFFITH†

(*Received* 22 *September* 1964 *and in revised form* 14 *January* 1965)

Abstract—A criterion is developed for bubble initiation from a gas filled cavity on a surface in contact with a superheated layer of liquid. It is found that the temperature of bubble initiation on a given surface is a function of the temperature conditions in the liquid surrounding the cavity as well as the surface properties themselves. It is also found that the delay time between bubbles is a function of the bulk liquid temperature and the wall superheat, and is not constant for a given surface.

By consideration of the transient conduction into a layer of liquid on the surface, a thermal layer thickness is obtained. With this thickness and a critical wall superheat relation for the cavity, a bubble growth rate is obtained.

Bubble departure is considered and it is found that the Jakob and Fritz relation works as long as the true (non-equilibrium) bubble contact angle is used. At one gravity the primary effect of bubble growth velocity on bubble departure size is found to be due to contact angle changes.

NOMENCLATURE

(Dimensions in H, M, L, T, Θ; the Heat Energy, Mass, Length, Time and Temperature).

L, latent heat of evaporation of fluid, [H M^{-1}];
P, pressure in the fluid outside the bubble, [$ML^{-1} T^{-2}$];
R, radius of bubble, [L];
R_c, radius of cavity, [L];
R_d, departure radius of bubble, [L];
S, bubble surface, [L^2];
T, temperature, [Θ];
T_b, temperature of vapor in the bubble, [Θ];
T_{sat}, saturation temperature of fluid at system pressure [Θ];
T_w, wall temperature, [Θ];
T_∞, temperature of main body of fluid, [Θ];
c, specific heat of fluid, [$HM^{-1} \Theta^{-1}$];
f, frequency of bubble generation, [T^{-1}];
g, gravity acceleration, [LT^{-2}];
h, coefficient of heat transfer from wall to the fluid, [$HT^{-1} L^{-2} \Theta^{-1}$];
h_v, coefficient of heat transfer from wall to vapor, [$HT^{-1} L^{-2} \Theta^{-1}$];
α, thermal diffusivity of fluid, [$L^2 T^{-1}$];
p, pressure inside the bubble, [$ML^{-1} T^{-2}$]
r, normalized bubble radius;
t, time, [T];
t_d, departure period, [T];
t_{ub}, unbinding period, [T];
t_w, waiting period, [T];
δ, thermal layer thickness, [L];
θ, $T - T_{sat}$; angle, [Θ];
μ, coefficient of viscosity, [$MT^{-1} L^{-1}$];
ν, kinematic viscosity, [$L^2 T^{-1}$];
ρ, density of fluid, [ML^{-3}];
ρ_v, density of vapor, [ML^{-3}];
σ, surface tension of fluid, [MT^{-2}];
τ, normalized time variable;
ϑ, volume of bubble, [L^3];
φ, angle of contact in static condition;
φ_b, base factor;
φ_c, curvature factor;
φ_s, surface factor;
φ_v, volume factor;
$\bar{\varphi}$, angle of contact in dynamic condition.

* Senior Engineer, Research & Development Division, Royal McBee Corporation, West Hartford, Connecticut.
† Associate Professor of Mechanical Engineering, Massachusetts Institute of Technology, Cambridge, Massachusetts.

Subscripts

d,	departure;
nc,	natural convection;
sat,	saturation;
ub,	unbinding;
w,	wall; waiting.

INTRODUCTION

THE PROCESS of nucleate boiling is the sum total of the processes of bubble initiation, growth and departure. Though there has been much study in the past few years of these individual processes, it has not been possible to tie together these various phenomena into a prediction of the heat flux–temperature difference relationship for a boiling surface. It has been necessary, when developing the boiling correlations, to assume some empirical relationship such as a power relating the heat flux to the temperature difference. When such an assumption was made, one was never sure that perhaps an implicit assumption of a possible bubble departure mechanism was not being made at the same time. The purpose of this work is to solve as best we can the heat flux–temperature difference relationship for one particular boiling experiment in order to see:

1. How much information had to be specified to make the solution possible.
2. How good the obvious geometric idealizations would be in making such predictions for the heat flux–temperature difference relationship.

It will soon be evident that the procedures used here are far too complicated to be of use in prediction in a practical problem, yet they will show what is necessary to complete the formulation of a boiling problem.

1. BUBBLE INITIATION THEORY

a. *General description*

A bubble is generally initiated from a small gas filled cavity or crack on the heating surface so long as the surrounding fluid is heated to a sufficiently high temperature. Both the preexistence of the gas phase and a sufficiently high wall temperature are necessary but they are not sufficient. The mechanism for bubble initiation has been discussed in reference 1 for the case of homogeneous temperature field. An extension of this mechanism to the nonhomogeneous temperature field (which is of primary interest) will be developed in this section. This problem was considered previously in reference 2, with the principal difference between this work and reference 2 in the geometric idealizations made in the bubble shape and the idealizations in the heat-transfer problem.

b. *Transient thermal layer*

Since the convection intensity near a solid wall is damped down due to the no-slip boundary condition for a solid surface, the use of the pure conduction equation is justified in determining the temperature distribution in a thin layer of fluid near the heating surface. Let us consider what the temperature distribution will be in the vicinity of the surface in the period of time after a bubble has departed and cold liquid has come in. If one treats the liquid as a solid slab the usual transient conduction equation applies. The initial and boundary conditions are shown in equations (1) and (2) below.

Initial condition is

$$\left.\begin{aligned} T &= T_w \quad \text{at} \quad x = 0 \\ T &= T_\infty \quad \text{at} \quad x > 0 \end{aligned}\right\} t = 0 \tag{1}$$

Boundary condition is

$$\left.\begin{aligned} T &= T_w \quad \text{at} \quad x = 0 \\ T &= T_\infty \quad \text{at} \quad x = \infty \end{aligned}\right\} t > 0 \tag{2}$$

The solution to this problem is

$$T - T_\infty = (T_w - T_\infty)\,\text{erfc}\,\frac{x}{2(at)^{1/2}} \tag{3}$$

$$\frac{\partial T}{\partial x} = -\frac{T_w - T_\infty}{(\pi a t)^{1/2}}\exp\left[-x^2/4at\right] \tag{4}$$

at $x = 0$

$$\left(\frac{\partial T}{\partial x}\right)_{x=0} = -\frac{T_w - T_\infty}{(\pi a t)^{1/2}} \tag{5}$$

If the actual temperature distribution near the wall is assumed to be a straight line distribution, the slope of this straight line is determined by equation (5). This assumption has been justified through measurements made in reference 3.

With this fact, one can introduce the notion of thickness of transient thermal layer by drawing a tangent line from $x = 0$ on the $T_w - T_\infty$ vs x curve defined by (3), the interception of this straight line on x-axis gives the transient thermal layer thickness.

$$\delta = (\pi \alpha t)^{1/2} \tag{6}$$

This means that the temperature distribution at any instant varies linearly from the wall to $x = \delta$. Beyond this the fluid is unaffected by the temperature of the wall. The layer thickness increases with the square root of the waiting time.

c. *Criterion of bubble growth initiation*

Having the definition of the transient thermal layer, one can determine the time required from the beginning of generation of thermal layer to the beginning of bubble growth. This period is defined as the waiting period of a bubble, t_w. The criterion for initiating bubble growth is from reference 4 and is that the thermal layer surrounding the bubble nucleus must be at a mean temperature equal to or above the temperature of the vapor in the bubble. This gives rise to an inward flow of heat from the superheated thermal layer to the bubble through the bubble wall. Before the bubble growth begins, the bubble is in a condition of thermostatic equilibrium. The equation of static equilibrium for the bubble is then

$$\Delta P = \frac{2\sigma}{R_c} \tag{7}$$

With the help of the Clausius–Clapeyron thermodynamic equilibrium relation, one has

$$\Delta P = \frac{\Delta T}{T_{\text{sat}}} \frac{L}{(1/\rho_v) - (1/\rho)} \approx \frac{\Delta T \, \rho_v L}{T_{\text{sat}}} \tag{8}$$

where

$$\Delta T = T_b - T_{\text{sat}}$$
$$\Delta P = P_b - P_{\text{sat}}$$

T_b, P_b are temperature and pressure of the vapor in the bubble at the initial stage of bubble growth.

Eliminating $\Delta\rho$ from above equations yields

$$\left.\begin{aligned} \Delta T = T_b - T_{\text{sat}} = \frac{2\sigma T_{\text{sat}}}{R_c \rho_v L} \\ \text{or} \\ T_b - T_\infty = T_{\text{sat}} - T_\infty + \frac{2\sigma T_{\text{sat}}}{R_c \rho_v L} \end{aligned}\right\} \tag{9}$$

During the waiting period when the bubble is hardly growing, it can be treated as an insulated hemispherical surface of radius R_c. Presumably there is tangential conduction in a thin layer around the bubble so that the interface temperature is also constant. The bubble consists for all practical purposes of an isothermal, adiabatic surface. A physical model of this idealization is shown in Fig. 1. In the following calculation only the adiabatic condition will be satisfied. From potential flow theory and the fluid flow analogy, the potential line in fluid flow is just equivalent to the isothermal line in heat conduction, the distance of an isothermal line passing through the top point of a waiting bubble is 3/2 R_c distant from heating surface when measured on the flat portion of this isothermal surface.

Fluid temperature at $x = 3/2\ R_c$ is

$$T_f = (T_w - T_\infty)\left[1 - \frac{(3/2)\ R_c}{\delta}\right] + T_\infty$$
$$= T_w - (T_w - T_\infty)\frac{3R_c}{2\delta} \tag{10}$$

Equating this temperature to the bubble temperature yields the criterion of initiation of bubble growth from a nucleate site of cavity radius R_c as

$$T_{\text{sat}} + \frac{2\sigma T_{\text{sat}}}{R_c \rho_v L} = T_w - (T_w - T_\infty)\frac{3R_c}{2\delta} \tag{11}$$

or

$$\delta = 3/2 \frac{(T_w - T_\infty) R_c}{T_w - T_{\text{sat}}[1 - (2\sigma/R_c \rho_v L)]}$$

when δ is expressed in terms of the waiting period

$$t_w = \frac{\delta^2}{\pi\alpha} = \frac{9}{4\pi\alpha}\left\{\frac{(T_w - T_\infty) R_c}{T_w - T_{\text{sat}}[1 + (2\sigma/R_c \rho_v L)]}\right\}^2 \tag{12}$$

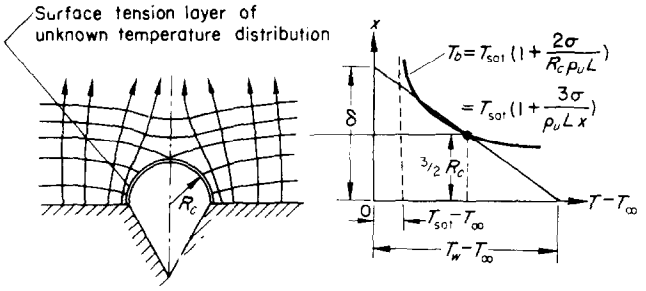

FIG. 1. Temperatures of fluid and bubble near a heating surface.

d. *The most favorable cavity radius for initiating bubble growth and the minimum waiting period*

As the waiting time increases, the thermal layer increases until at a certain condition the temperature line of fluid becomes tangent to the bubble equilibrium temperature curve. At this instant and if, and only if, there is a gas filled cavity of radius R_{cf} on the heating surface, a bubble will begin to grow from this spot. This radius, corresponding to a minimum waiting period, is called the most favorable cavity radius R_{cf}. Let us now turn our attention to the solution of equation (11).

Solving for R_c for (11) yields

$$R_c = \frac{\delta (T_w - T_{sat})}{3 (T_w - T_\infty)} \left\{ 1 \pm \left[1 - \frac{12 (T_w - T_\infty) T_{sat}\, \sigma}{(T_w - T_{sat})^2\, \delta\, \rho_v L} \right]^{1/2} \right\} \tag{13}$$

For any given waiting period, there are two possible cavity radii—any cavity filled with gas and with radius bounded by these two radii will nucleate. When these two cavity radii are equal, it means the two intersecting points coincide (see Fig. 2), or the fluid temperature line and bubble equilibrium temperature curve are tangent to each other. Observing (13) gives the condition of equal roots of R_c as

$$1 - \frac{12 (T_w - T_\infty) T_{sat}\, \sigma}{(T_w - T_{sat})^2\, \delta\, \rho_v L} = 0$$

Solving for δ which is by definition δ_{min}, yields

$$\delta_{min} = \frac{12 (T_w - T_\infty) T_{sat}\, \sigma}{\rho_v L (T_w - T_{sat})^2} \tag{14}$$

Equal root condition is (13) with help of (14) gives

$$\left.\begin{aligned} R_{cf} &= \frac{\delta_{min} (T_w - T_{sat})}{3 (T_w - T_\infty)} = \frac{4 T_{sat}}{T_w - T_{sat}} \frac{\sigma}{\rho_v L} \qquad \text{(a)} \\ (t_w)_{min} &= \frac{\delta_{min}^2}{\pi a} = \frac{144 (T_w - T_\infty)^2 T_{sat}^2\, \sigma^2}{\pi a\, \rho_v^2 L^2 (T_w - T_{sat})^4} \qquad \text{(b)} \end{aligned}\right\} \tag{15}$$

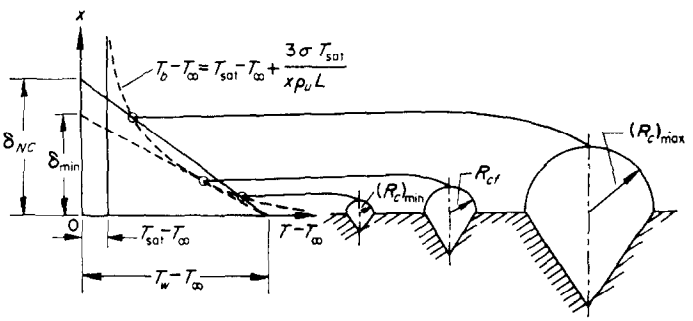

FIG. 2. Initiation of bubble growth from different cavities.

e. *Upper and lower bounds of radius of active nucleate cavity*

The thermal layer cannot, in general, increase without limit with the waiting time. It will be washed off by the natural convection of the fluid as it grows beyond the thickness of natural convection layer δ_{nc}. This means

$$\delta_{\max} = \delta_{nc} \tag{16}$$

Knowing $\delta_{\max}$ from the natural convection information, the maximum and minimum cavity radius for initiating a bubble growth can can be calculated from (13) with the help of (16)

$$(R_c)_{\max;\,\min} = \frac{\delta_{nc}\,(T_w - T_{\text{sat}})}{3\,(T_w - T_\infty)} \left\{ 1 \pm \left[1 - \frac{12\,(T_w - T_\infty)\,T_{\text{sat}}\,\sigma}{(T_w - T_{\text{sat}})^2\,\delta_{nc}\,\rho_v L} \right]^{1/2} \right\} \tag{17}$$

Any cavity outside this interval cannot qualify as an active nucleation site. A cavity of radius greater than $(R_c)_{\max}$ will be finally deactivated by the invasion of the surrounding fluid, since the gas pressure inside the cavity is not sufficient to maintain a stable equilibrium with the surface tension of the fluid. A diagram is shown in Fig. 2. Experimental verification of these and other equations will be presented later in this paper.

2. BUBBLE GROWTH THEORY

a. *Assumptions*

(i) Neglect any convection, not due to the bubble itself.

(ii) Neglect the loss of mass of the fluid due to evaporation or condensation through the interface of vapor and liquid.

(iii) Convert the one dimensional case into a three dimensional case by the introduction of a curvature factor.

(iv) Neglect the inertia force and the surface tension of the fluid in their effect on the pressure in the bubble.

(v) Assume constant properties for the fluid.

(vi) Assume a spherical bubble surface.

(vii) Assume a uniform wall temperature and uniform bulk fluid temperature and a uniform fluid pressure.

After waiting period t_w, the bubble will grow. For the first few moments, the surface tension effects and the inertia effects of surrounding fluid are so large that the growth rate is controlled by momentum equation; but after the radius increases to about twice its initial value, the surface tension and inertia effects will become negligible, and the growth rate is controlled by the heat transfer. In this study, only the heat-transfer effects will be considered in the evaluation of bubble growth curve.

b. *Formulation and solution*

For clarification, the one dimensional physical model for heat-transfer mechanism is illustrated in Fig. 3.

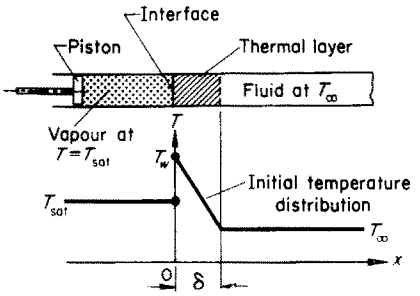

FIG. 3. Simplified physical model of heat transfer.

Initial condition is

$$\left.\begin{aligned} &T = T_w - (T_w - T_\infty)\frac{x}{\delta} \text{ for } 0 < x < \delta \\ &\text{where} \qquad \delta = (\pi\alpha\, t_w)^{1/2} \\ &T = T_\infty \qquad \text{for } \delta < x < \infty \end{aligned}\right\} t = 0 \tag{18}$$

Boundary condition is

$$\left.\begin{aligned} T &= T_{\text{sat}} \quad \text{for } x = 0 \\ T &= T_\infty \quad \text{for } x = \infty \end{aligned}\right\} t > 0 \tag{19}$$

Introducing a new variable

$\theta = T - T_{\text{sat}}$ such that

$$\theta_{\text{sat}} = 0,\ \theta_w = T_w - T_{\text{sat}},\ \theta_\infty = T_\infty - T_{\text{sat}} \tag{20}$$

then (18) and (19) are transformed to

$$\left.\begin{aligned} \theta &= \theta_w - \frac{\theta_w - \theta_\infty}{\delta} x \quad \text{for} \quad 0 < x < \delta \\ \theta &= \theta_\infty \qquad\qquad\qquad \text{for} \quad \delta < x < \infty \end{aligned}\right\} t = 0 \tag{21}$$

and

$$\left.\begin{aligned} \theta &= 0 \quad \text{for} \quad x = 0 \\ \theta &= \theta_\infty \quad \text{for} \quad x = \infty \end{aligned}\right\} t > 0 \tag{22}$$

The governing equation is then

$$\frac{\partial^2\theta}{\partial x^2} = \frac{1}{\alpha}\frac{\partial\theta}{\partial t} \tag{23}$$

The problem is now reduced to a semi-infinite conductor, with a prescribed initial temperature $\theta(x, 0) = f(x)$ and surface temperature zero; then the solution of (23) with conditions (21) and (22) is as follows.

$$\theta = \frac{1}{2(\pi\alpha t)^{1/2}} \int_0^\infty f(x') \{\exp[-(x - x')^2/4\alpha t] - \exp[-(x + x')^2/4\alpha t]\}\, dx' \tag{24}$$

where

$$\begin{aligned} f(x') &= \theta_w - \frac{\theta_w - \theta_\infty}{\delta} x' \quad \text{for} \quad 0 < x' < \delta \\ &= \theta_\infty \qquad\qquad\qquad\quad \text{for} \quad \delta < x' < \infty \end{aligned}$$

$$\frac{\partial\theta}{\partial x} = \frac{-1}{4(\pi)^{1/2}(\alpha t)^{3/2}} \int_0^\infty f(x') \{(x - x') \exp[-(x - x')^2/4\alpha t] - (x + x') \exp[-(x + x')^2/4\alpha t]\}\, dx' \tag{25}$$

at $x = 0$ (25) becomes

$$\begin{aligned} \left(\frac{\partial\theta}{\partial x}\right)_{x=0} &= \frac{1}{4(\pi)^{1/2}(\alpha t)^{3/2}} \int_0^\infty f(x')(2x') \exp[-x'^2/4\alpha t]\, dx' \\ &= \frac{1}{2(\pi)^{1/2}(\alpha t)^{3/2}} \left\{ \int_0^\delta x' \left(\theta_w - \frac{\theta_w - \theta_\infty}{\delta} x'\right) \exp[-x'^2/4\alpha t]\, dx' + \int_\delta^\infty \theta_\infty x' \exp[-x'^2/4\alpha t]\, dx' \right\} \\ &= \frac{1}{(\pi\alpha t)^{1/2}} \left(\theta_w - \frac{\theta_w - \theta_\infty}{\delta} (\pi\alpha t)^{1/2} \operatorname{erf} \frac{\delta}{(4\alpha t)^{1/2}}\right) \end{aligned} \tag{26}$$

Referring to the bubble growth model as shown in Fig. 4, the governing equation for bubble growth is

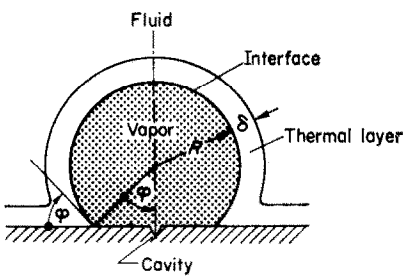

FIG. 4. Simplified model of bubble growth.

$$\rho_v \left(4\pi R^2 \frac{dR}{dt}\right) \varphi_v L = \varphi_c \varphi_s (4\pi R^2) ac\rho \left(\frac{\partial\theta}{\partial x}\right)_{x=0} + \varphi_b (4\pi R^2) h_v (T_w - T_{sat})$$

or

$$\frac{dR}{dt} = \frac{\varphi_c \varphi_s}{\varphi_v} \frac{ac\rho}{\rho_v L} \left(\frac{\partial\theta}{\partial x}\right)_{x=0} + \frac{\varphi_b h_v (T_w - T_{sat})}{\varphi_v \rho_v L} \tag{27}$$

where $\varphi_c =$ curvature factor where $1 < \varphi_c < 3^{1/2}$

$$\varphi_s = \text{surface factor} = \frac{2\pi R^2 (1 + \cos\varphi)}{4\pi R^2} = \frac{1 + \cos\varphi}{2}$$

$$\varphi_b = \text{base factor} = \frac{\pi R^2 \sin^2\varphi}{4\pi R^2} = \frac{\sin^2\varphi}{4}$$

$$\varphi_v = \text{volume factor} = \frac{\frac{1}{3}(4\pi R^3) - \frac{1}{3}[2\pi R^3(1 - \cos\varphi)] + \frac{1}{3}\pi R^3 \sin\varphi\cos\varphi}{\frac{1}{3}(4\pi R^3)} \tag{28}$$

$$= \frac{2 + \cos\varphi\,(2 + \sin^2\varphi)}{4}$$

$\varphi =$ contact angle

$h_v =$ coefficient of heat transfer from heating surface to the steam bubble through its base area.

Substituting (26) into (27) yields

$$\frac{dR}{dt} = \frac{\varphi_c \varphi_s}{\varphi_v} \frac{ac\rho}{\rho_v L} \frac{1}{(\pi at)^{1/2}} \left(\theta_w - \frac{\theta_w - \theta_\infty}{\delta} (\pi at)^{1/2} \operatorname{erf} \frac{\delta}{(4at)^{1/2}}\right) + \frac{\varphi_b h_v \theta_w}{\varphi_v \rho_v L} \tag{29}$$

For the case of a bubble growing in an infinite fluid field of superheat θ_w then $\varphi_s = 1$, $\varphi_v = 1$, $\varphi_b = 0$, $\varphi = 0$, $\delta = \infty$ and (29) becomes

$$\frac{dR}{dt} = \frac{\varphi_c ac\rho}{\rho_v L} \frac{\theta_w}{(\pi at)^{1/2}} = \frac{\varphi_c}{\pi^{1/2}} \frac{\theta_w \rho c}{\rho_v L} \left(\frac{a}{t}\right)^{1/2} \tag{30}$$

From homogeneous solution of bubble growth rate, one has from the growth theory summarized in reference 4

$$\frac{dR}{dt} = \left(\frac{3}{\pi}\right)^{1/2} \frac{\theta_w \rho c}{\rho_v L} \left(\frac{a}{t}\right)^{1/2} \tag{31}$$

Comparing (30) and (31), one finds the value of curvature factor to be

$$\varphi_c = 3^{1/2} \quad \text{for} \quad \varphi = 0 \quad \text{and} \quad \delta \gg R \tag{32}$$

Another extreme case is for $\varphi = \pi$, it reduces exactly to one dimensional case then

$$\varphi_c = 1 \tag{33}$$

For $\varphi = 0$, $\delta \ll R$, it reduces to the thin thermal layer case which was also summarized in reference 4.

$$\varphi_c = \frac{\pi}{2} \tag{34}$$

Combining these three extreme cases, one can manufacture a φ_c such that it satisfies (32), (33), and (34) simultaneously, i.e.

$$\varphi_c = \left[3^{1/2} + \frac{\varphi}{\pi}(1 - 3^{1/2})\right]\left[\left(1 - \frac{\varphi}{\pi}\right)\frac{(\pi/2\,3^{1/2})\,\bar{R} + \delta}{\bar{R} + \delta} + \frac{\varphi}{\pi}\right] \tag{35}$$

This is an approximate expression which satisfies the known asymptotic conditions and is smooth and continuous between these conditions. Where $\bar{R}$ is the time average of bubble radius or

$$\bar{R} \equiv (1/t)\int_0^t R\,dt \tag{36}$$

Integrating (29), with respect to time t gives

$$R - R_c = \frac{\varphi_s\,\varphi_c}{\varphi_v}\frac{ac\rho}{\rho_v L}\int_0^t \frac{1}{(\pi a t)^{1/2}}\left[\theta_w - (\theta_w - \theta_\infty)\frac{(\pi a t)^{1/2}}{\delta}\operatorname{erf}\frac{\delta}{(4at)^{1/2}}\right]dt + \frac{\varphi_b\,h_v\,\theta_w}{\varphi_v\,\rho_v L}\,t$$

or

$$R - R_c = \frac{\varphi_s\,\varphi_c}{\varphi_v}\frac{ac\rho}{\rho_v L}\left[\frac{2\theta_w}{(\pi a)^{1/2}}\,t^{1/2} - \frac{\theta_w - \theta_\infty}{\delta}\frac{\delta^2}{4a}\left(\frac{4at}{\delta^2}\operatorname{erf}\frac{\delta}{(4at)^{1/2}} + \frac{2}{(\pi)^{1/2}}\frac{(4at)^{1/2}}{\delta}\exp\left[-\delta^2/4at\right] - 2\operatorname{erfc}\frac{\delta}{(4at)^{1/2}}\right)\right] + \frac{\varphi_b\,h_v\,\theta_w}{\varphi_v\,\rho_v L}\,t \tag{37}$$

Normalizing (37) by introducing dimensionless variables

$$\tau = \frac{4at}{\delta^2} \quad \text{and} \quad r = \frac{R}{\delta} \quad \text{leads to}$$

$$r - r_c = \frac{\varphi_s\,\varphi_c}{\varphi_v}\frac{c\rho\theta_w}{\rho_v L}\left[\left(\frac{\tau}{\pi}\right)^{1/2} - \frac{\theta_w - \theta_\infty}{\theta_w}\left(\tau\operatorname{erf}\frac{1}{\tau^{1/2}} + \frac{2}{\pi^{1/2}}\,\tau^{1/2}\exp\left(-1/\tau\right) - 2\operatorname{erfc}\frac{1}{\tau^{1/2}}\right)\right] + \frac{\varphi_b\,\delta\,h_v\,\theta_w}{4\,\varphi_v\,\rho_v L a}\,\tau \tag{38}$$

A bubble growth plot for $T_\infty > T_{\text{sat}}$, $T_\infty = T_{\text{sat}}$ and $T_\infty < T_{\text{sat}}$ in normalized coordinates is shown in Fig. 5.

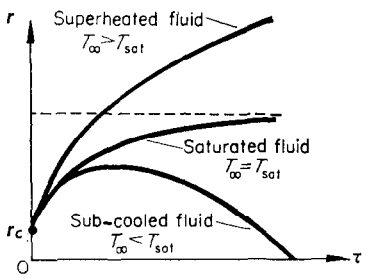

FIG. 5. Normalized bubble growth curves.

c. *Discussion of the bubble growth theory*

In the bubble growth theory, the thermal layer on the bubble surface is assumed to be picked up by a growth of bubble immediately at the last moment of waiting period. From the high-speed photographic study to be described, one can see that in the first moments, the bubble growth rate is very high and the bubble expands laterally at such a rate that, in fact, a very large piece of thermal layer is picked up during the

first few moments. This fact gives a strong support to the one dimensional approach. Actually, the bubble growth history is composed of three periods, namely the waiting period t_w, the unbinding period t_{ub}, and the departure period t_d. When the wall superheat increases, the waiting period of bubble at a particular cavity decreases very rapidly. If the thermal layer thickness calculation is still based on the waiting period, the error will be very large. This will make the deviation between the theoretical bubble growth rate and actual one also very large. From Fig. 6, in which the dynamic effect and surface tension effects to bubble

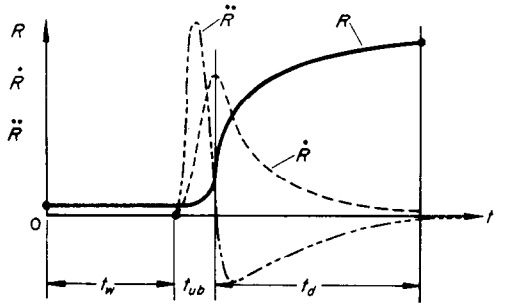

FIG. 6. Bubble growth curve when the dynamic effects and surface tension are considered.

growth are shown, the following can be seen: During the waiting period, the subcritical bubble is heated in order to initiate growth from its cavity. During unbinding period, the bubble is trying to liberate itself from the binding force of surface tension and the inertia effects of the surrounding fluid. The bubble radius increases very slowly and the momentum equation governs the motion of bubble surface. During the departure period, the effects of surface tension and inertia of fluid become so small that the heat-transfer equation governs the motion of bubble surface the the thermal layer is picked up by the growing bubble immediately during the first few moments of this period. Therefore the thermal layer thickness for very high wall superheat case where the waiting period is very short should be calculated by $\delta = [\pi\alpha(t_w + t_{ub})]^{1/2}$ instead of $\delta = (\pi\alpha\, t_w)^{1/2}$. Observations from those 22 bubbles listed in Table 4 show that the departure period was nearly constant, the waiting period changed by a factor eight to one. The uneven heating due to a 500 watt light source for photography purpose at the rear side of test section caused a pronounced unsymmetrical turbulent convection of fluid which changed the thermal layer distribution. The temperature fluctuations associated with this turbulence gave rise to fluctuations in the waiting period also.

3. BUBBLE DEPARTURE

A number of possible limiting processes can be responsible for the departure size actually observed in an experiment. The most obvious of these is that departure occurs when the size of the bubble gets so large it is not possible to satisfy a vertical gravity–surface tension force balance on the bubble. In the experiments reported later in this paper it was found, indeed that this was the condition which led to bubble departure; the only proviso being that for a rapidly growing bubble, the dynamic rather than static contact angle must be used. This picture of bubble departure is essentially that of Fritz [5], and the relation he proposed for bubble departure is

$$R_d = 0{\cdot}4251\ \varphi \left(\frac{2\sigma}{g(\rho - \rho_v)}\right)^{1/2} \tag{39}$$

When a bubble grows so that R becomes greater than R_d, the bubble departs.

4. BUBBLE INITIATION, GROWTH AND DEPARTURE AND THE BUBBLE FREQUENCY

Using experimental values for the contact angle, as measured from the tracings presented later, one can use equation (39) to solve for the departure size. Equation (37) can then be used to solve for the time to departure t_d. The waiting time, t_w, can be found from equation (12). The frequency then becomes

$$f = \frac{1}{t_w + t_d} \tag{40}$$

A bubble generation and departure cycle diagram is shown in Fig. 7.

5. EXPERIMENTAL PROGRAM

The purpose of the experiments was to check the bubble initiation, growth and departure theories. For this purpose the apparatus described below was constructed.

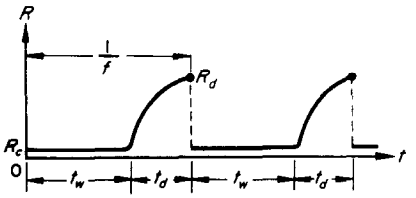

FIG. 7. Bubble generating cycles.

a. *Experimental set-up*

The experimental set-up is shown in some detail in Figs. 29 and 30 of reference 5. The heating surface was made by electroplating a layer of 16 ct gold of 0·005 in thickness on the top surface of a thin flanged cylindrical copper block. The heated surface was 1·1875 inches in diameter. The reason for gold plating was to minimize the effects of oxidation so that the surface conditions would remain the same from the beginning to the end of each test. At the bottom of copper block, seven 120 W Chromelux electrical heaters were imbedded in holes in the copper block. The heat generated by these heaters was transferred to the top surface by pure conduction. The reduction of cross section of copper block underneath the heating surface was for the purpose of intensifying the heat flux at the heating surface. A thin flange surrounds the heater to eliminate undesired bubble nucleation which might occur at a boundary. This flange was very thin so that the temperature near the edge of the heating surface was low enough to prevent bubble initiation. A piece of Teflon heat insulator was inserted between the lower face of this thin flange and pool base. A Thermos-bottle filled with ice was used for the cold junction of the thermocouples which were connected with a potentiometer through a six-way switch. A drain hole valve was also attached to the bottom of the test section. In order to predict the surface temperature, three thermocouples T_1, T_2, and T_3 were inserted in the holes on the shank part of the copper block, a three point interpolation formula was used to determine the wall temperature T_w. These thermal couple holes were $\frac{1}{16}$ inch in diameter, $\frac{19}{32}$ inch in depth and were spaced $\frac{1}{4}$ in apart. All dimensions were measured from the heating surface. The bottoms of these three holes were at the center line of the shank. In the fluid, another thermocouple, T_4, was used to measure the temperature of main body of fluid, T_∞. It was located one inch above the heating surface. All thermocouples were made of No. 30 chrome-alumel wire. In order to avoid excessive corrosion, the thermocouple T_4 was shielded in a $\frac{1}{16}$ in stainless steel tube with Teflon seal at the outer end.

The fluid was contained in a 3 in diameter and 20 in length, specially heat-treated, high strength glass tube. Observations and photographs could be made through a so-called "fluid crystal". This was a glass box filled with the same fluid as that in testing section and so placed as to eliminate distortion due to curvature. The front wall was flat, the rear wall was made of a segment of circular tube with a radius of curvature just equal to the outside radius of the testing tube, such that the distortion of bubble shape due to light refraction of tube was eliminated. With this device, an accurate measurement of the bubble dimensions could be obtained from high-speed photography.

A helically wound copper tube in the upper part of the testing tube was used as a condenser. The saturation temperature of the fluid T_{sat} was controlled by varying the system pressure from 1 atm to $\frac{1}{4}$ atm through an asperator vacuum pump. The temperature of the main body of fluid T_∞ was controlled by varying the flow rate of the cooling water through a cock. The wall temperature T_w was controlled by varying the electrical power of the heaters through a Variac.

b. *Surface preparation*

Boiling data are difficult to reproduce due to changes in the surface conditions. There are two ways in which these changes appear; namely, changes due to contamination and to cavity reactivation. Contamination can be eliminated by proper choice of the metal for the heating surface; reactivation of a nucleate cavity can be eliminated by the following method.

The 16 ct gold plated surface was first finished by 200 grit emery paper which was continuously wetted by a water jet. The direction of stroke was kept constant. The surface was finished by stroking in one direction until all scratches were eliminated, then rotating 90° to eliminate all the scratches in the other direction. The whole

piece was then washed in a water jet. Following exactly the same procedure, the surface was finished by 400 grit and 600 grit emery paper. The surface was then cleaned by hot water jet, alcohol jet and hot air jet and was then put on the No. 4 diamond compound wheel. The diamond compound should be put on the center area of the grinding wheel and diluted by kerosene before starting grinding operation. The piece was held gently near the edge area of wheel, kerosene was injected on the wheel cloth occasionally. Operation was continued until the scratches due to 600 grit emery paper disappeared completely. Then the piece was taken off the No. 4 diamond compound wheel, the hot water jet, the alcohol jet and the hot air jet were then each put on the surface. After the washing process, the piece was then put on the No. 6 diamond compound wheel and then No. 8 wheel using the same sequence of operations as on the No. 4 wheel.

At the last few minutes of grinding process on the No. 8 diamond compound wheel, the kerosene jet was applied all over the center area of the wheel, such that the diamond compound was washed to a very dilute condition, the piece was then put near the center part of the wheel where the rubbing speed is lower, then a heavier pressure was applied. After 1–2 min. the surface would become shining, mirror-like smooth. It was washed by hot water jet, alcohol jet and hot air jet; it was then introduced in the pool of an ultrasonic cleaner for 2 min. This process would help to wash out small diamond dust particles and bits of metal which were trapped in the cavities on the surface. Then the surface was washed again by alcohol and methyl ether jet. The surface at this stage was assumed to be the surface required.

After each test, the surface was renewed by going through all the steps immediately after No. 6 diamond compound wheel.

In order to keep surface condition unchanged, every element which is in the boiling system should be cleaned by washing soap, hot water jet and distilled water jet before each test.

c. *Method of experimentation*

After making a new surface and washing all the parts, they were assembled, distilled water was introduced into the top of the test section. Two hours of vigorous boiling with a moderate heat flux was maintained for degassing purposes, then the heat flux was reduced until there were no active cavities on the surface, then the heat flux was increased gradually until the first active cavity appeared on the surface. This was the starting point of each test. A steady state condition was assumed to be reached 2 h after the heat flux was changed.

During each run the following measurements were made:

Power, fluid temperature, heater-unit temperatures, system pressure, number of active centers, and number of new sites arising from the change in heat flux. Technically the latter are called the initiated cavities which generate bubbles with very low frequencies so that the contribution to the heat transfer is negligible. The heat transfer to the fluid through the heating surface was determined by the simple conduction formula knowing the temperature gradient in the shank of the copper block. The wall temperature T_w within a circular area of 1·1875 in diameter on the center part of the heating surface was assumed to be uniform.

d. *Photographic technique*

High-speed photographs were taken with a Wollensack camera. A Kodak Tri-X negative 100′ film for high-speed photography was used. About 2400 frames per second were taken which necessitated a reduction of voltage supplied to the Wollensack camera motor to about 70 V through a Variac. A 500 W illumination lamp was installed at the rear of the test section about 6 in away from the tube center, so that the heating surface looked shining bright. The focus of the camera was very carefully adjusted so that no relative motion between the circle on the focusing lens and the bubble to be photographed was observed.

The camera was placed as close as possible to the test section without losing the sharp focus required. A reference wire of 0·040 inches in diameter was placed beside the bubble which was to be photographed. The bubble diameter measurements were made by projection on a microfilm projector. A geometric mean value of bubble diameters in two principal axis

directions was considered as the bubble diameter for volume calculation.

e. *Heat flux determination and surface temperature prediction*

Heat flux was determined by differentiation of the thermocouple readings and surface temperature was determined by extrapolating these readings to the surface.

6. EXPERIMENTAL RESULTS

The diameters and shapes of the first three bubbles were obtained in detail from a single high-speed motion picture film during which simultaneous measurements of heat flux and surface temperature were made. From the same film the waiting periods for these bubbles and a number of others were also obtained. The measured shapes are presented in Figs. 8, 9, and 10. Figure 11 is a plot of the measured radius time curves. The diameters are tabulated in Tables 1, 2 and 3 and the history of delay times and departure times summarized in Table 4. It is now possible to make a comparison of these quantities with the preceding theory.

Table 1. Bubble growth

The experimental data for bubble Number 1
$t_w = 0{\cdot}0245$ s.
$t_d = 0{\cdot}0166$ s.
$R_d = 3{\cdot}974 \times 10^{-3}$ ft
Camera speed = 1140 frames/s.

No. of frame	t (ms)	Bubble diameter on microfilm projector (mm) scale = 8·87:1	R (mft)
1	0	2·32	0·429
2	0·877	9·48	1·754
3	1·654	13·72	2·538
4	2·631	16·04	2·967
5	3·508	17·80	3·293
6	4·385	18·40	3·404
7	5·262	18·95	3·506
8	6·139	19·57	3·620
9	7·016	19·86	3·674
10	7·893	20·00	3·700
11	8·770	20·36	3·767
12	9·647	20·72	3·833
13	10·524	21·10	3·904
14	11·401	21·65	4·005
15	12·278	21·90	4·052
16	13·155	21·90	4·052
17	14·032	21·80	4·033
18	14·909	21·69	4·013
19	15·786	21·48	3·974 (R_d)

Table 2. Bubble growth

The experimental data for bubble Number 2
$t_w = 0{\cdot}0437$ s.
$t_d = 0{\cdot}0167$ s.
$R_d = 5{\cdot}328 \times 10^{-3}$ ft
Camera speed = 1260 frames/s.

No. of frame	t (ms)	Bubble diameter on microfilm projector (mm) scale = 8·87:1	R (mft)
1	0·793	9·26	1·713
2	1·586	14·22	2·631
3	2·379	17·53	3·243
4	3·172	19·76	3·656
5	3·965	21·65	4·005
6	4·758	22·80	4·218
7	5·551	23·87	4·416
8	6·344	24·67	4·564
9	7·137	25·20	4·662
10	7·930	25·48	4·714
11	8·723	25·50	4·718
12	9·516	25·80	4·773
13	10·309	26·10	4·829
14	11·102	26·74	4·947
15	11·895	27·26	5·043
16	12·688	27·40	5·069
17	13·481	27·70	5·125
18	14·274	27·90	5·162
19	15·067	28·53	5·278
20	15·860	28·87	5·341
21	16·653	28·80	5·328 (R_d)

For the data tabulated in this section, no direct verification of the bubble nucleation mechanism is possible. However, it can be said that the delay times t_w are larger than that $(t_w)_{\min}$ as given by equation (14) so these readings are not incompatible with what has been said about the mechanism of bubble nucleation. The missing measurement is the cavity size. For these experiments they were too small to measure directly and the necessary information about the temperature difference at the inception of boiling was not obtained. It was originally hoped to put cavities of a known size on the surface, but it was not found possible to get the surface smooth enough so as to force bubble nucleation to occur only from the desired points. In a succeeding paper, this nucleation theory will be assumed to be correct and will be used to com-

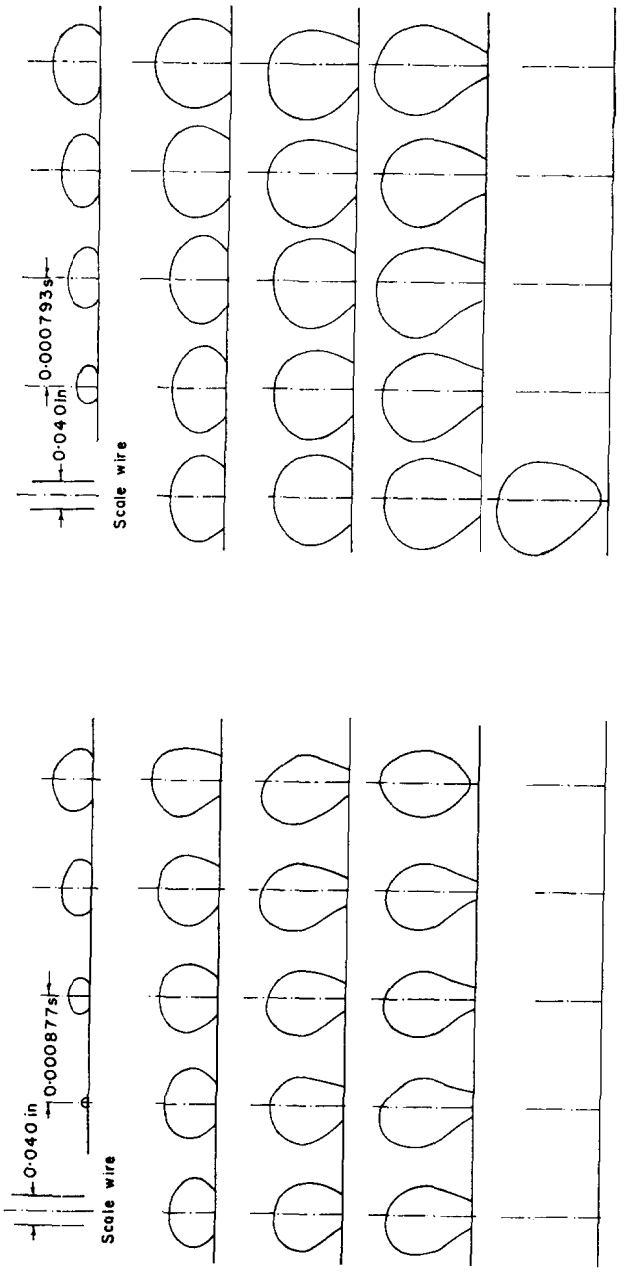

FIG. 8. History of growth of bubble Number 1.

FIG. 9. History of growth of bubble Number 2.

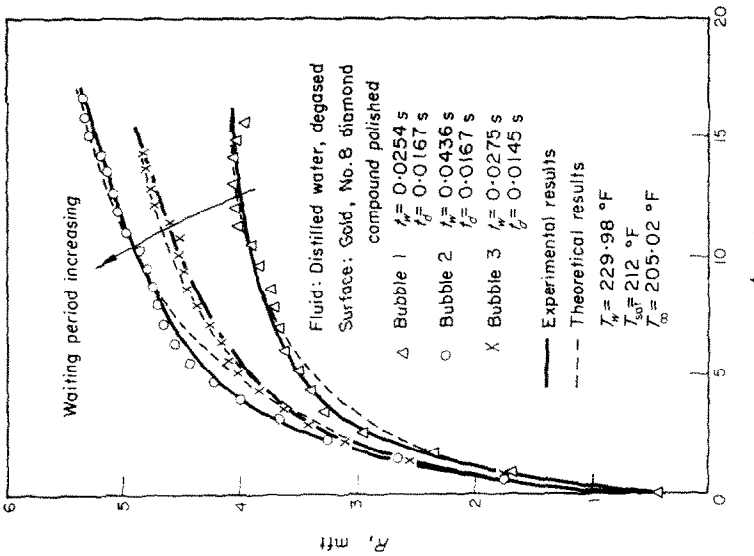

FIG. 11. Bubble growth plot.

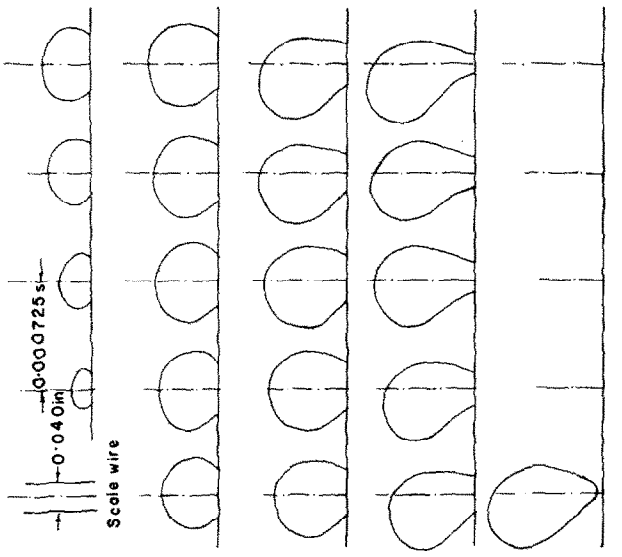

FIG. 10. History of growth of bubble Number 3.

Table 3. Bubble growth

The experimental data for bubble Number 3
$t_w = 0{\cdot}0275$ s.
$t_d = 0{\cdot}0145$ s.
$R_d = 0{\cdot}395 \times 10^{-3}$ ft
Camera speed = 1380 frames/s.

No. of frame	t (ms)	Bubble diameter on microfilm projector (mm) scale = 8·87:1	R (mft)
1	0·725	9·52	1·711
2	1·450	14·10	2·609
3	2·175	16·88	3·123
4	2·900	18·45	3·413
5	3·625	19·55	3·617
6	4·350	20·60	3·811
7	5·075	21·73	4·020
8	5·800	22·08	4·085
9	6·525	22·53	4·168
10	7·250	22·75	4·209
11	7·975	23·68	4·381
12	8·700	24·00	4·440
13	9·425	24·10	4·459
14	10·150	24·33	4·501
15	10·875	24·15	4·468
16	11·600	24·74	4·577
17	12·325	25·52	4·721
18	13·050	25·80	4·773
19	13·775	25·88	4·788
20	14·500	25·90	4·792 (R_d)

Table 4. History of bubble generations

$T_w = 229{\cdot}98$°F, $T_{sat} = 212$°F, $T_\infty = 205{\cdot}02$°F
Distilled water on gold surface ground by No. 8 diamond compound

Bubble no.	Camera speed frames/s	t_w (s)	t_d (s)	R_d (mft)
1	1140	0·0254	0·0167	3·974
2	1260	0·0436	0·0167	5·328
3	1380	0·0275	0·0145	4·792
4	1500	0·0466	0·0167	3·534
5	1650	0·0735	0·0261	3·691
6	1800	0·0594	0·0172	4·224
7	1920	0·0490	0·0151	4·188
8	2040	0·0633	0·0162	4·658
9	2130	0·0319	0·0155	3·931
10	2190	0·0337	0·0160	5·125
11	2280	0·0672	0·0149	3·321
12	2370	0·0785	0·0167	3·448
13	2520	0·1640	0·0143	3·633
14	2700	0·1250	0·0512 (Three in tandem)	4·201
15	2770	0·0436	0·0143	3·566
16	2850	0·0393	0·0161	4·782
17	2910	0·0216	0·0158	5·367
18	2910	0·0450	0·0139	3·374
19	2940	0·0756	0·0296 (Two in tandem)	3·571
20	2940	0·0252	0·0163	4·967
21	2940	0·0354	0·0139	3·883
22	2940	0·0490	0·0129	4·183

Observation from above table shows that the waiting period t_w changes from $17(t_w)_{min}$ to $130(t_w)_{min}$.

pute a heat-transfer rate temperature difference relation. The comparison with experiment there will provide some additional indirect verification for these bubble nucleation ideas.

Bubble growth can be computed without an arbitrary constant by use of the observed delay times. Equation (6) gives the thermal layer thickness, while equation (38) gives the radius time curve. A comparison of the theory and experiments is shown in Fig. 11.

In making the comparisons between theory and experiment, measured contact angles and measured delay times are used. Neither of these quantities was constant from bubble to bubble as can be seen from an examination of Table 4. This randomness has been observed before in boiling processes [7], and is apparently inherent in it. Because of this, the favorable comparison between theory and experiment as shown in Fig. 11 is partly fortuitous. It is felt that this randomness is due to the fact that at the conditions at which these measurements were made bubble nucleation was marginal. This meant that large fluctuations in bubble history resulted from relatively small turbulent fluctuations in the temperature conditions around the bubbles. An exact prediction of what is going to occur in such a situation does not appear to be possible.

A comparison of the theory and experiment for bubble departure for the same three bubbles using the receding contact angle is presented in Fig. 12. The comparison here is satisfactory. A plot of receding contact angle vs mean bubble growth rate is given in Fig. 13. There is a casual relationship between the two which will be needed to predict boiling performance in part two of this paper. In reference 8 systematic deviations between the bubble size at departure and the predictions of equation (39) were

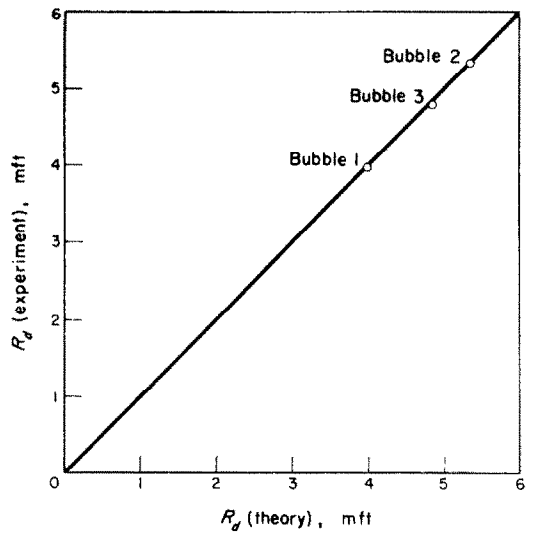

FIG. 12. Verification of bubble departure theory.

observed if the bubbles were changing size at the time. It is felt from an examination of the data taken in these experiments that these deviations were a result of an attempt to use a single mean contact angle for the whole bubble growth and departure process. If the appropriate receding contact angle were used, it is felt that most of the velocity dependence of departure size on growth rate would disappear.

7. CONCLUSIONS

(a) Bubble growth and departure, at least for pool boiling at low heat flux, are well understood, though exact predictions are not possible due to inherent randomness in part of the process.

(b) Bubble nucleation is understood in principle except that direct measurement of cavity size was not possible, so that an arbitrary constant had to be used in the interpretation of the bubble nucleation data.

(c) Bubble nucleation from a given site has a rather irregular period due apparently to the random differences in the temperature of the water coming in after a bubble departs.

8. DISCUSSION

Implicit in the equations describing the bubble nucleation process is the assumption that the process is periodic, with a regular period. As can be seen in Table 4, this is hardly the case. The most likely explanation for this is that the temperature difference is scarcely more than the minimum necessary to nucleate bubbles in these experiments and the effect on the bubble frequency of a slightly lower temperature turbulent fluctuation is very large. For higher wall superheats the delay time between bubbles would be more probably regular, but the delay would

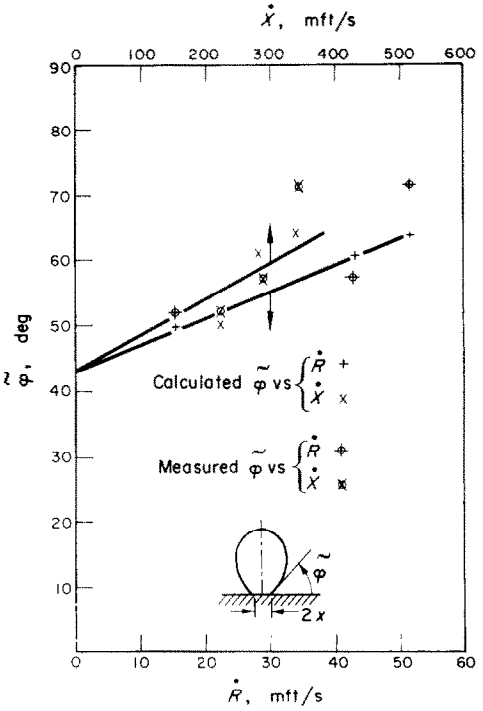

FIG. 13. The dynamic effect of bubble growth rate to contact angle.

certainly be shorter. The precision of measuring these short delays is very small; therefore the conditions reported represent a compromise between the conflicting requirements of a reproducible and of an accurate delay time measurement.

The correlation between the measured and calculated growth rates and departure sizes is as good as can be expected within the inherent randomness of the process. It can be concluded that, with respect to these processes there is no longer any hidden physics.

It is appropriate at this point to consider some of the other processes which may lead to bubble departure, as the Fritz mechanism is clearly not the only one possible. If the contact angle is very small, the bubble cannot depart until the rise velocity is greater than the growth velocity. In a flowing system the bubbles are perhaps drawn off the surface by hydrodynamic lift. If there is a little subcooling in the liquid, it appears that the bubble can "spring" off the surface due to dynamic effects. Apparently the momentum imparted to the liquid ahead of the bubble draws the bubble off if its growth decelerates rapidly enough. There are perhaps other mechanisms for bubble departure too. In a different geometry or under different conditions any one of these processes might be limiting. The analytical description of these processes would also differ.

ACKNOWLEDGEMENTS

This work has been entirely supported by the Office of Naval Research and has been performed in the Heat Transfer Laboratory of the Massachusetts Institute of Technology, which is under the direction of Professor W. M. Rohsenow.

We express appreciation for the help and suggestions of Professor W. M. Rohsenow and Professor Moissis throughout the past three years. Thanks are due also to Professor Rightmire and Professor Argon for their suggestions on surface preparation.

REFERENCES

1. P. GRIFFITH, The role of surface conditions in nucleate boiling, *A.I.Ch.E., Symposium Series*, August (1959).
2. Y.-Y. HSU, On the size range of active nucleation cavities on a heating surface, *J. Heat Transfer* **84**, (1962).
3. T. A. CLARK, Pool boiling in an accelerating system, *ASME*, Paper No. 60-*HT*-22.
4. L. E. SCRIVEN, On the dynamics of phase growth, *Chem. Engng Sci.* **10**, 1–13 (1959).
5. W. FRITZ, Berechnung des maximal Volumens von Dampfblasen, *Phys. Z.* **36**, 379 (1935).
6. C.-Y. HAN, The mechanism of heat transfer in nucleate pool boiling, Sc.D. Thesis, M.I.T. (1962).
7. P. H. STRENGE, A. ORELL and J. W. WESTWATER, *J. Amer. Inst. Chem. Engrs* **7**, 578–583 (1961).
8. B. E. STANISZEWSKI, Nucleate boiling bubble growth and departure, Technical Report No. 16, *DSR* Project No. 7-7673, M.I.T., August (1959).

Résumé—On expose un critère pour la formation de bulles à partir d'une cavité remplie de gaz sur une surface en contact avec une couche surchauffée de liquide. On trouve que la température de formation de bulles sur une surface donnée est une fonction des conditions de température dans le liquide entourant la cavité aussi bien que les propriétés de surface elles-mêmes. On trouve aussi que la durée entre les bulles successives est une fonction de la température globale du liquide et de la surchauffe de la paroi et n'est pas constante pour une surface donnée.

En considérant la conduction transitoire dans une couche de liquide sur la surface, on obtient une épaisseur de couche thermique. Avec cette épaisseur et une relation critique de surchauffe de paroi pour la cavité, on obtient une vitesse de croissance de bulle.

On considère le détachement de la bulle et on trouve que la relation de Jakob et Fritz est valable aussi longtemps qu'on emploie le vrai angle de contact (en non-equilibre). Pour une gravité unité, on trouve que le principal effet de la vitesse de croissance des bulles sur la taille des bulles au détachement est due aux changements de l'angle de contact.

Zusammenfassung—Für das Entstehen von Blasen aus einer mit Gas gefüllten Vertiefung an einer Oberfläche in Berührung mit einer überhitzten Flüssigkeitsschicht wird ein Kriterium entwickelt. Es ergab sich, dass die Temperatur beim Blasenentstehen an einer gegebenen Oberfläche eine Funktion der Temperaturbedingungen in der Flüssigkeit ist, die die Vertiefung ebenso wie die Oberflächenbeschaffenheiten selbst umgibt. Es zeigte sich ebenfalls, dass die Verzögerungszeit zwischen den Blasen eine Funktion der Flüssigkeitstemperatur und der Wandüberhitzung und keine Konstante für eine gegebene Oberfläche ist.

Unter Berücksichtigung der Ableitung in eine Flüssigkeitsschicht an der Oberfläche erhält man eine thermische Schichtdicke. Mit dieser Dicke und einer Beziehung der kritischen Wandüberhitzung für die Vertiefung erhält man eine Blasenwachstumsgeschwindigkeit. Das Ablösen der Blasen wird beobachtet und dabei gefunden, dass die Beziehung von Jakob und Fritz solange gilt, wie der wahre (nicht im Gleichgewicht befindliche) Randwinkel der Blase eingesetzt wird. Bei Normalschwere findet man, dass der primäre Einfluss der Blasenwachstumsgeschwindigkeit auf die Ablösegrösse der Blasen von Veränderungen des Randwinkels hervorgerufen wird.

Аннотация—Получен критерий зарождения пузырьков в заполненной газом полости на поверхности, соприкасающейся со слоем перегретой жидкости. Найдено, что температура зарождения пузырьков на данной поверхности является функцией температурных условий в жидкости, окружающей полость, а также самих свойств поверхности. Найдено также, что частота отрыва пузырьков является функцией объемной температуры жидкости и перегрева стенки и не постоянна для данной поверхности.

Путем рассмотрения нестационарной теплопроводности слоя жидкости на поверхности получена толщина термического слоя. Зная эту толщину и соотношение перегрева стенки для полости, можно получить скорость роста пузырька.

Рассмотрен отрыв пузырьков и найдено, что соотношение Якоба и Фритца справедливо до тех пор, пока применяется истинный (неравновесный) угол контакта пузырьков (краевой угол смачивания поверхности). Найдено, что при отрыве под действием одной лишь силы тяжести, основное влияние скорости роста пузырька на отрывной его диаметр обязано изменениям угла контакта.